Dissociation of C 1s excited states of OCS

Christian Stråhlman

June 8, 2009

Degree project (Bachelor of Science), 15 hp

Supervisor: Stacey Sörensen
Assistant supervisors: Denis Ceolin and Joakim Laksman

Division of Synchrotron Radiation Research
Department of Physics

LUND UNIVERSITY
Faculty of Science

Abstract

Excitation of the C 1s core-electron in carbonyl sulfide (OCS) gives rise to many dissociation channels. Excitation at the C 1s edge gives rise to localized core-holes in carbon atoms, thus being strongly site specific. Photoelectron–photoion coincidence (PEPICO) measurements of the fragmentation of OCS have been done with 3D spectroscopy at MAX-lab in Lund. I show in this report strong differences between the behavior of the O=C bond and the C=S bond by an analysis of the energy and dissociation directions of the molecular fragments O^+ and S^+. The C=S bond is hereby found to be weaker than the O=C bond. I also show the existence of alignment effects when OCS is irradiated by plane polarized synchrotron radiation corresponding to the C 1s – π^* excitation and the C 1s – σ^* excitation. The present report in addition provides an overview of the basic molecular orbital theory.

Acknowledgments

I would say that one of the biggest success-factors of a degree project is supporting supervisors and co-workers. And I have certainly not lacked any of that.

I would like to express my gratitude to all co-workers at the Division of Synchrotron Radiation Research for all support. I found a division with a very including atmosphere and helpful people. You have made this, sometimes extremely hectic, semester into something I have really enjoyed.

I would like to thank my assistant supervisors: Joakim Laksman, who showed me everything I wanted to know about the experimental setup and who has continuously upgraded and enhanced all computer scripts I have been working with; and Denis Ceolin, who supervised me when this report was compiled and who has helped me to understand the theoretical framework.

To the rest of the research group I say thanks for all interesting discussions around the coffee-table each Monday afternoon. It has given me a sense of the diversity of this subject and the research going on which I could not imagine when I started this.

And to Stacey Sörensen, my supervisor – I am extremely grateful that I got the opportunity to join you and your group for this project. Your support has been immensely important for me. You're simply the best!

FIGURE 1 – *The OCS molecule.*

Populärvetenskaplig sammanfattning

I alla tider och på alla platser har människan försökt förstå hur världen hänger ihop. Sökandet efter den substans som bygger världen har lett oss till upptäckterna av molekylerna, atomerna och atomernas byggstenar. Och när man tränger längre och längre in i materiens märkligheter finner man att svaren inte bara ligger i vad byggstenarna är, utan också hur de trivs med varandra. Växelverkan – hur partiklar visar för varandra vilka de är och var de finns – gör att materian kan sluta sig samman i strukturer som bygger universum.

Den som vill förstå hur en samling atomer kan sättas ihop till alla material som vi omger oss med måste förstå hur atomerna sitter ihop. Vi måste veta hur atomerna beter sig när de är tillsammans. Vi vill veta hur atomerna föredrar att placera sig, och vad som händer när de blir störda.

I det här arbetet har jag studerat en liten molekyl som består av tre atomer. Karbonylsulfid (OCS) består av tre atomer som sitter på rad. Molekylen är mycket nära släkt med koldioxid (CO^2), man har bara bytt ut en syreatom mot en dubbelt så tung svavelatom. Svavelatomer och syreatomer är kemiskt väldigt lika. Man kan i många molekyler byta ut en syreatom mot en svavelatom utan att molekylens form ändras. Men eftersom svavelatomen är större och dubbelt så tung som syreatomen bör det finnas skillnader. OCS blir intressant att studera eftersom man har med både syre och svavel i var sin ända av molekylen.

När en foton (en liten bit ljus) absorberas av en molekyl kan det innebära att en elektron får mer energi än tidigare (den exciteras). Fotonens energi flyttas från fotonen till elektronen. Jag har studerat vad som händer om man exciterar en elektron som är mycket hårt bunden till kolatomen så att den nästan blir helt fri. Man bestrålar molekylen med röntgenstrålning som man får från en synkrotronljuskälla. Ljusets energi går då över till elektronen i kolatomen. Den exciterade elektronen flyttar då ut från mitten av atomen till en position i utkanten. När molekylen har så mycket extra energi så är den inte stabil. Molekylen kommer att innehålla mycket överflödig energi som den måste göra sig av med. Många gånger går en sådan molekyl sönder i två eller flera delar (fragment). Genom att mäta vilka fragment som bildas och hur de rör sig kan man ta reda på mer om hur atomerna satt ihop från första början.

Jag kan i detta arbete visa att bindningen mellan kol och syre är starkare än den mellan kol och svavel. Därför går molekylen hellre sönder där. Jag visar också att bindningen mellan kol och syre går sönder bara om OCS-molekylen blir av med minst två elektroner.

Contents

1 Introduction

The present report is the written part of my diploma work in physics (FYSK01; Diploma work for bachelor degree in Physics), which is the result of the degree project I have laid my efforts on during the spring-term 2009. The workload of this project is equivalent to 15 higher education credits, and it has been carried out part-time during the whole semester.

In this project I have, besides writing this report, joined the research group lead by Stacey Sörensen in their daily work. I have in particular participated in the preparations for their beam-time at beam-line I411 at MAX-lab in February 2009. These preparations gave me experiences in working with synchrotron radiation, setting up a vacuum system, aligning a detector and much more. I have had the opportunity to inspect and observe all three storage rings at MAX-lab, and how they work. Hence, I have been familiarized, hands-on, with all the experimental equipment in this report. The experimental setup used for the beam-time in February was the same as used when the data in this report was acquired. All experimental data in this report was acquired by Stacey Sörensen's research group at I411 at MAX-lab in November 2008.

All computerized analysis has been performed using the MATLAB-script *ANACONDA*, developed by Joakim Laksman.

This report has been publicly presented and defended at June 1st, 2009.

2 Theory

In this section I will outline relevant theory to understand and interpret the dissociation channels presented later in this text.

2.1 Electronic structure of molecules

To find and understand the electronic structure of molecules one must generalize the mechanics of the simple atomic system to apply on a system containing more than one nucleus. Although the atomic system is well known, a generalization to molecules has proven to be far more complex. One major feature in determining molecular structure is the increasing number of degrees of freedom as two atoms combine to form a molecule. Since an atom is considered to be a sphere it has no fixed direction in space and complete symmetry in all directions. Thus all properties dependent of direction are degenerate in the atom. A molecule however has a direction. Furthermore the molecular properties are dependent of the interatomic distances. As the atom just concerns itself with translational motion, a molecule can rotate and vibrate.

In the atom electrons are distributed among atomic orbitals (AO). These are characterized by their principal quantum number n and their orbit quantum number l. The orbit quantum number determines the shape of the orbital, see *figure 2*. The orbitals all have a maximum number of electrons which they can contain due to the Pauli principle.

In the thought experiment where two atoms are moved close to each other, orbitals interfere with each other and combine into molecular orbitals (MO). These orbitals hold the key to bonding mechanisms. Especially the covalent bonding, which keeps most molecules together, is explained by molecular orbital theory.

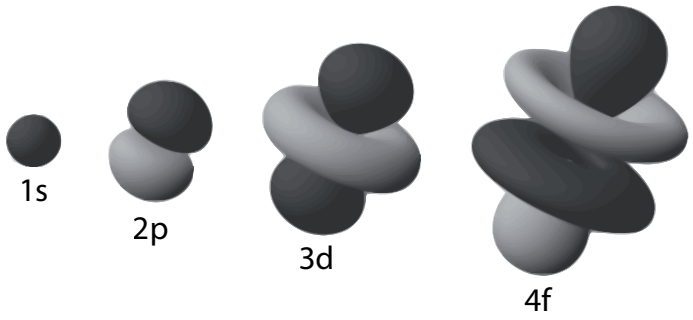

FIGURE 2 – *Characteristic shape of the s, p, d, f atomic orbitals. The illustration also shows in black and grey where the atomic wave function has the same sign (positive or negative). When constructing molecular orbitals with the LCAO technique, a bonding orbital is formed when two atomic orbitals overlap and the overlapping parts have the same sign. If they have different signs, the molecular orbitals are anti-bonding. Since the signs of the atomic orbitals are interchangeable a bonding and an anti-bonding orbital always forms together, although there might be that only one of them is occupied.*

As in the atomic case, the total electronic wave function is a product function [1][2].

$$\Psi = \Phi_1 \Phi_2 \ldots \Phi_n \tag{1}$$

The spatial part of each Φ is the molecular orbital. To acquire such orbitals, one possible method is to uses the MO-LCAO method (Molecular Orbitals as Linear Combinations of Atomic Orbitals). As the name implies, one uses existing atomic orbitals, combines them and use the result as a molecular orbital. Consider an atomic orbital ϕ_a in atom A and an atomic orbital ϕ_b in atom B. The molecular orbital(s) arising from these atomic orbitals has the form

$$\Phi = c_a \phi_a + c_b \phi_b \tag{2}$$

where c_a, c_b are constants. If more than two atomic orbitals participate in the molecular orbital it can be written as a sum over atomic orbitals

$$\Phi_k = \sum_i c_i \phi_i \tag{3}$$

One can build a molecular theory in this way by considering first one-electron molecules and then increase complexity to more electrons and more nuclei. In the present text, this will not be done since it will only concern bonding and orbital shape.

Consider two atoms merged together into a molecule. The ground configuration of each atom is well known. Electrons are situated in orbitals designated by $s, p, d, f \ldots$, all with different shape and/or direction. The atoms dealt with in this paper – O, C and S – do only consist of s- and p-orbitals.

As seen in *figure* 2, s-orbitals has spherical symmetry (i.e. no particular direction in space). p-orbitals have a characteristic hour glass shape and thus a direction in

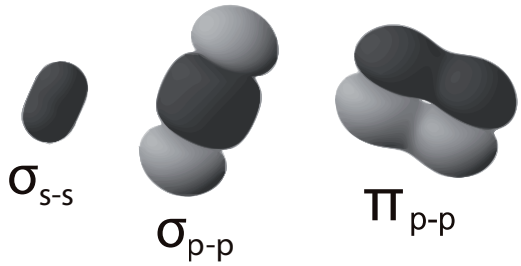

FIGURE 3 – *Examples of the simplest molecular orbitals where two nuclei are bonded. From left to right: (1) σ bonding orbital with two s atomic orbitals participating. (2) σ bonding orbital with two p_z atomic orbitals participating. (3) π anti-bonding orbital with two $p_{x,y}$ orbitals participating. This orbital is identified as anti-bonding since it has a node-plane in between the nuclei perpendicular to the bonding axis. Note also that this orbital lacks cylindrical symmetry.*

space. Three perpendicular p-orbitals are designated by p_x, p_y, p_z. When these orbitals participate in bonding, convention is to let the z-axis coincide with the bonding axis (i.e. the line connecting the nuclei). The p-orbital wave function is positive in one lobe and negative in the other.

Molecular orbitals can be designated by Greek letters ($\sigma, \pi, \delta, \phi \ldots$) in a similar fashion as atomic orbitals ($s, p, d, f \ldots$).

1. If the orbital has rotational symmetry in respect to the bond-axis, it is a σ-orbital.
2. If the orbital has one node plane[1] parallel to the bond-axis, it is a π-orbital.
3. If the orbital has two, three... node planes parallel to the bond-axis, it is a $\delta, \phi \ldots$)-orbital.

If $\Phi = 0$ the probability of finding an electron in that point is equal to $|\Phi|^2 = 0$. An electron in a π-orbital can thus never be found exactly on the bond-axis. One can draw further conclusions of the properties of an orbital by using node planes.

1. If the orbital has a node plane perpendicular to the bond-axis in between the nuclei, it is an anti-bonding orbital.
2. If the orbital has no such node plane, it is a bonding orbital.

One possible way to explain covalent bonding is in terms of columbic attraction and repulsion. Electrons attract atomic nuclei, other nuclei do not. If two nuclei are brought close to each other, they will repulse each other. However, if an amount of negative charge is brought in between, nuclei will bond together and stay close. The

[1] A node plane is a plane which intersect the orbital in such a way that the orbital wave function $\Phi \equiv 0$ for all intersecting points.

trick is to form a state where electrons have a high probability to be found in between the nuclei. Such a state would be "bonding". The opposite case, where electrons have a low probability to be found in between the nuclei, would be "anti-bonding".

When creating an orbital in accordance with the MO-LCAO-method one simply adds wave functions together. Consider, for example, two s-orbitals. The s-orbital has a wave function that does not change sign. Thus, $|\phi(\mathbf{r})|^2 > 0 \, \forall \mathbf{r}$. However, ϕ can be a positive or a negative function. The linear combination is

$$\Phi = c_a \phi_a + c_b \phi_b. \tag{4}$$

If both terms carry the same sign it is clear that $|\Phi(\mathbf{r})|^2 > 0 \, \forall \mathbf{r}$, and thus there is a higher probability for the electron to be between the nuclei than to be anywhere else. In the opposite case, when the terms have opposite signs, Φ must also change sign, and the molecular orbital Φ must have a node-plane between the nuclei. This lowers the probability to find the electron between the nuclei.

This implies that when one wants to create molecular orbitals, one takes two or more orbitals that have overlapping wave functions. If the overlapping functions have equal signs, the electron probability rises in this region and a bond is formed. A bonding molecular orbital is formed. If the signs are opposite, the electron probability is lowered in the region. An anti-bonding molecular orbital is formed. An electron in the bonding orbital always has lower energy than an electron in a participating atomic orbital, and vice versa.

The molecular orbital formed above is a σ-orbital since it has rotational symmetry. σ-orbitals is also formed when two p_z-orbitals or one s and one p_z combine. s and p_z cannot combine with p_x and p_y since the overlap has same and opposite signs in equal parts. Two p_x or two p_y can however combine. These will form π-orbitals.

Bonding orbitals created in this manner are considered to be covalent bonds. Characteristic for covalent bonds is the sharing of electrons among the bonded atoms. This is natural when one considers that molecular orbitals stretch over both atoms in the bond. Since each atomic orbital can contain two electrons (spin direction), and the same rule applies to molecular orbitals, each pair of atomic orbitals must give rise to a pair of molecular orbitals. That is true since there is both bonding and anti-bonding orbitals created.

2.2 The OCS molecule

The OCS molecule is in its ground state a triatomic linear molecule. Chemically, the atom is held together by two double bonds between the carbon atom and the sulfur and oxygen atom respectively. OCS is thus closely related to CO_2 and CS_2, which in the same way are bonded by two double bonds. The difference is symmetry properties. CO_2 and CS_2 are symmetric through their central carbon atom, thus belonging to the $D_{\infty v}$ symmetry group[2]. OCS, not carrying this property, belongs to the $C_{\infty v}$ symmetry group[3]. OCS has 30 electrons distributed as follows[7]:

$$(1\sigma)^2(2\sigma)^2(3\sigma)^2(4\sigma)^2(5\sigma)^2(1\pi)^4(6\sigma)^2(7\sigma)^2(8\sigma)^2(2\pi)^4(9\sigma)^2(3\pi)^4$$

Of the 30 electrons in OCS, 14 are core electrons, namely

$$(\mathrm{S}\,1\mathrm{s})^2(\mathrm{O}\,1\mathrm{s})^2(\mathrm{C}\,1\mathrm{s})^2(\mathrm{S}\,2\mathrm{s})^2(\mathrm{S}\,2\mathrm{p})^6$$

[2]Cylindrical symmetry
[3]Conical symmetry

corresponding to

$$(1\sigma)^2(2\sigma)^2(3\sigma)^2(4\sigma)^2(5\sigma)^2(1\pi)^4$$

Thus the three S 2p-orbitals consists of one σ-orbitals and two π-orbitals[4]. The rest of the electrons occupy valence levels.

Core-electrons in molecules do not participate in bonds. Therefore they are localized to their respective nuclei. They are also characterized by high binding energies[5], e.g. 290 eV for the C 1s electron. Valence electrons often participate in molecular bonds and are therefore much more delocalized (they stretch over the entire molecule). Since the valence electrons are 'outer electrons' by definition, they also possess lower binding energies (a few up to a few tenth eV).

The ordering of valence orbitals is identical in OCS, CO_2 and CS_2. Since these molecules are held together by double-bonds, one can draw the conclusion that 8 valence electrons participate in bonding, distributed among two σ- and two π-orbitals.

Above the filled orbitals there is an "infinite" series of unoccupied orbitals. The construction of the covalent bond is such that all anti-bonding orbitals in OCS are unfilled. Next in line must therefore be a number of anti-bonding orbitals. In the following, electrons will be promoted from core-levels up to these anti-bonding orbitals.

2.3 Photoabsorption

We have measurements where a core-electron in the carbon atom has been promoted to an empty valence level of the OCS molecule, namely a σ^*or π^*orbital, by absorption of a linearly polarized photon.

A transition, like the one mentioned above, is when a system, i.e. the molecule, undergoes a change from a initial state $|i\rangle$ to a final state $|f\rangle$. The transition probability can be expressed within the electric dipole approximation

$$P \propto |\mathbf{e} \cdot \langle f|\mathbf{r}|i\rangle|^2 .$$

Here $\mathbf{r}$ is the position of the electron which one excites, and $\mathbf{e}$ is the unit polarization vector of the linearely polarized light. *Lindgren* [4] discusses in his thesis the probability for this transition if one excites a 1s core-electron to a valence orbital by evaluating the matrix element $\langle f|\mathbf{r}|i\rangle$. One finds that the transition probability can be expressed as

$$P \propto |\mathbf{e} \cdot \mathbf{O}|^2$$

where $\mathbf{O}$ is the direction of the largest amplitude of the orbital which the electron is excited to. There is a strong dependence of orbital direction where transition is preferred when the electric vector of the light and the orbital points in the same direction.

The implication is that a σ-orbital has its largest amplitude along the internuclear axis. A transition from a 1s-orbital to a σ-orbital is therefore most likely when the molecular axis is paralell to the polarization vector. A π-orbital has its largest amplitude perpendicular to the internuclear axis. A transition from a 1s-orbital to a π-orbital is most likely when the orbital is aligned with the polarization vector.

[4]This is reasonable since the p_z-orbital is parallel to the molecular axis and p_x, p_y are perpendicular to the same.

[5]In this case the energy required to promote the specific electron to a position at infinite distance from the nuclei.

When this occur, the internuclear axis is perpendicular to the polarzation vector. There is however not always a high transition probability when the internuclear axis is perpendicular to the polarzation vector, since the π-orbital is not rotationally symmetric.

2.4 Core-excitation and dissociation

By exposing an OCS molecule to radiation which has an energy equal to a specific transition in the molecule one dramatically increases the probability for this transition to happen. This is to induce a resonant transition. In this project OCS has been exposed to radiation with energy corresponding to the energy of a transition where a core-electron is promoted to a valence orbital. The main difference of promoting a core-electron and a valence electron is that the core-electron is strongly localized in the molecule, i.e. site-specific. The promotion of a core-electron thus leaves the molecule with a core-hole which is localized to a specific nucleus. By applying different resonant energies, one can thus determine where a core-hole should be created.

Core-electron excitation implies that the molecule is put in a highly exited and unstable state. This is induced by the absorption of a light quantum

$$h\nu + X \rightarrow X^*$$

Such a state is very rapidly decaying. It is with conventional methods not possible to detect molecules with core-holes before decay. Since photon energies responsible for core-excitation are in the range of a few hundred eV, the molecule experiences a huge surplus energy which must be handled in some kind of process. The alternatives available are:

Photon emission — The surplus energy is transferred (partially or wholly) to a photon which is emitted.

Electron emission — The surplus energy is transferred to one (or more) of the electrons which is emitted, leaving the molecule in an ionized state.

Dissociation — The bonds breaks and the molecule breaks into dissociation fragments. The fragments can be two or more. Remaining surplus energy is transferred to translational motion of the fragments.

All these processes can happen in series. E.g. a molecule can first ionize one or two or more times, then dissociate into two or more fragments.

Consider OCS. Following core-excitation

$$h\nu + \mathrm{OCS} \rightarrow \mathrm{OCS}^*$$

ionization can take place

$$\mathrm{OCS}^* \rightarrow \mathrm{OCS}^{+(*)} + e^-$$

and possibly ionization once again

$$\mathrm{OCS}^{+*} \rightarrow \mathrm{OCS}^{++(*)} + e^-$$

and then there is the possibility of dissociation.

Since we are only able to detect charged fragments by this TOF-technique, we must make the assumption that the OCS molecule is ionized before dissociation. As we will observe, doubly and triply charged OCS must be considered. We expect that OCS dissociates into OC/S, O/CS and O/C/S with different distributions of charge among the fragments.

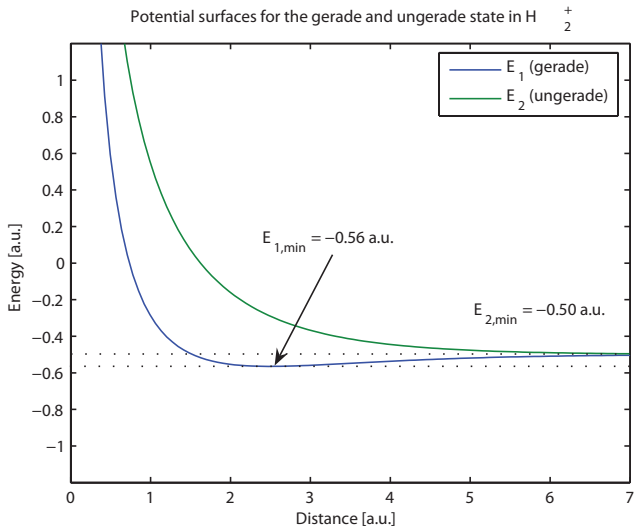

FIGURE 4 – *Potential surfaces of the two orbitals in the hydrogen molecular ion,* H_2^+

2.5 Molecular potential

All fragmentation processes must conserve momentum. When molecules dissociate, one reason they do so because of Coulomb repulsion of nuclei. The force that acts on the nuclei is directed along the bond axis. When two fragments are separated they gain momentum directed parallel to this force. This is also true when the linear OCS molecule dissociate into two fragments. To measure the momentum direction after fragmentation is to measure the initial alignment of the molecule. As we shall see, this can provide information on light absorption of the molecule.

Although nuclear repulsion is the general cause of dissociation it is necessary to consider molecular potentials to grasp the general idea of molecular dissociation. As two atoms are moved together they combine into a molecule, and we have previously seen that energy levels thereby are split. In some cases these are bonding orbitals and in some cases these are anti-bonding. What is actually the big difference? Since molecules, as almost all physical systems, tend to minimize energy, the equilibrium distance between atoms is decided by if there is a distance which has a local energy minimum. Bonding orbitals has this property; anti-bonding orbitals do not. It can be shown that the minimum energy for this system is at infinite separation.

In *figure 4* the potential surfaces of the two orbitals in the simplest molecule H_2^+ is shown. The minimum energy mentioned above is clearly seen, as well as the anti-bonding properties. Even if this is only a true calculation for the one electron case, the general idea is valid for more complex systems. The overall potential surface of the molecule can, after excitation, be such as it has no local energy minimum. Such a molecule will dissociate if a decay channel involving electronic transitions does not intervene.

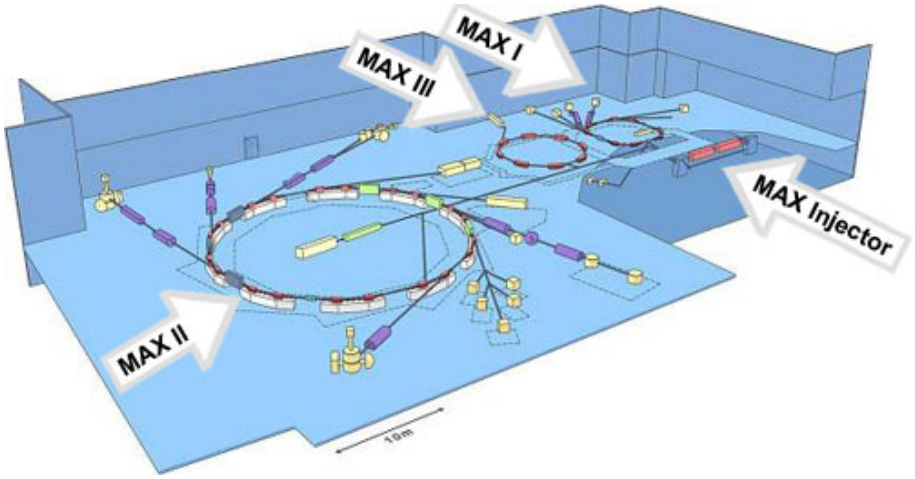

FIGURE 5 – *The MAX-lab synchrotron radiation facility in Lund. The experiments in this paper were performed on MAX II, beamline I411. [5]*

3 Methods

3.1 Synchrotron radiation

The idea that charged particles accelerated by direction change would emit radiation was considered already in 1898. The first visual observation of such radiation was in 1947, and the first experiments with the new kind of radiation were performed in 1956.

Electrons who's path is bent by a magnetic field will emit radiation with a wavelength determined by the speed of the electrons and the strength of the field[6]. Higher speed and stronger fields gives shorter wavelengths (higher photon energy).

In a synchtrotron radiation facility electrons are kept circulating in a storage ring. Synchrotron radiation facilities are considered to have undergone three phases – generations. First generation facilities were purely parasitic as synchrotron radiation researchers were using the radiation produced at facilities used for other purposes in atomic and nuclear physics. Second generation facilities were designed for the purpose of synchrotron radiation research. These facilities produced light solely by bending the electron paths so they circulated the ring. Third generation facilities – such as MAX-lab, *figure 5* – are circular just for the purpose to keep the electrons in the ring. The light is produced by insertion devices, such as undulators and wigglers. These devises (see *figure 6*) uses alternating magnetic fields to make the electrons oscillate along their trajectory. Photons are thus produced in each turn, making the efficiency considerably higher. As photons are emitted along the trajectory of the electron they all share the same direction. Also, they have the same polarization – plane, with polarization vector perpendicular to the magnetic field and the electron trajectory. When the electrons have passed the insertion device, they are bent to the next section of the storage ring. The light continue its propagation out of the storage ring and into the beamline.

[6]In practice, the field strength is determined by the curvature of the storage ring.

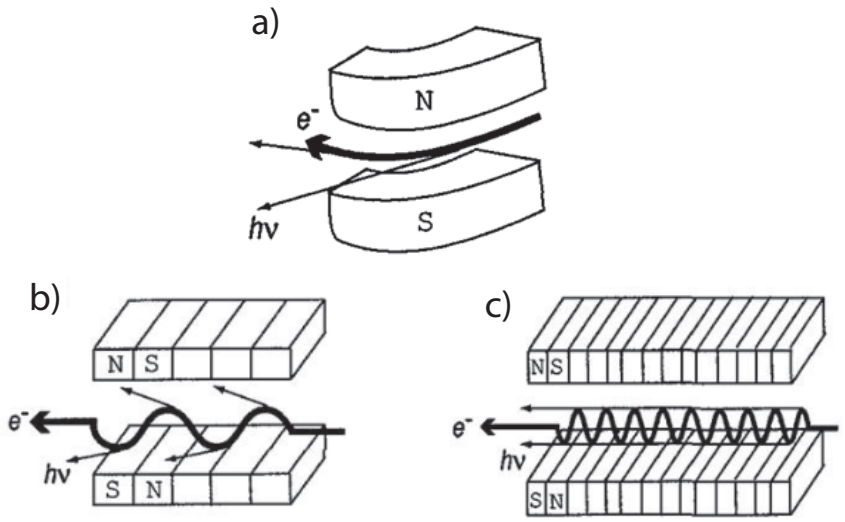

FIGURE 6 – *a) The electron is accelerated with a simple dipole magnet. Such acceleration produces radiation in an uncontrolled way and in a broad spectrum. b) Undulator. c) Wiggler – The electron is forced to oscillate in an alternating magnetic field. Radiation is emitted along the electron trajectory. [6]*

The experiments in this report has been performed with soft X-rays. Experiments were executed at MAX-lab in Lund, the Swedish national laboratory for synchrotron radiation research, at the beamline I411 (*figure 7*), which can produce photons in the energy range 40–1500 eV. This beamline is equipped with a undulator with tunable magnetic field. Thus, it is possible to create light with a specific energy. Together with a monochromator in the beamline light with a very narrow energy range is produced.

3.2 Time-of-flight and Photoelectron–Photoion Coincidence

In a homogeneous electric field a charged particle experiences a constant force parallel or anti-parallel to the field vector. These particles are subject to acceleration which, according to Newton's second law and the definition of the electric force, will be inversely proportional to their mass-to-charge ratio. Thus, the time it takes for a particle with zero initial kinetic energy to travel a certain distance in a homogeneous electric field will be solely determined by the mass-to-charge ratio of that particle. This is the argument that allows us to use time-of-flight spectrometers. If the initial kinetic energy of a certain ion is sufficiently low, we suspect all ions of that kind to have the same TOF. Hence, one is able to, under certain conditions, evaluate the mass-to-charge ratio of an unknown particle.

To evaluate TOF, one must design a detector which is able to record two events: One which starts the clock and one which stops it. The time interval recorded must also have a meaningful interpretation. The solution lies in the photoelectron–photoion coincidence (PEPICO) technique.

The TOF-spectrometer used to acquire the data in this paper consists primarily of

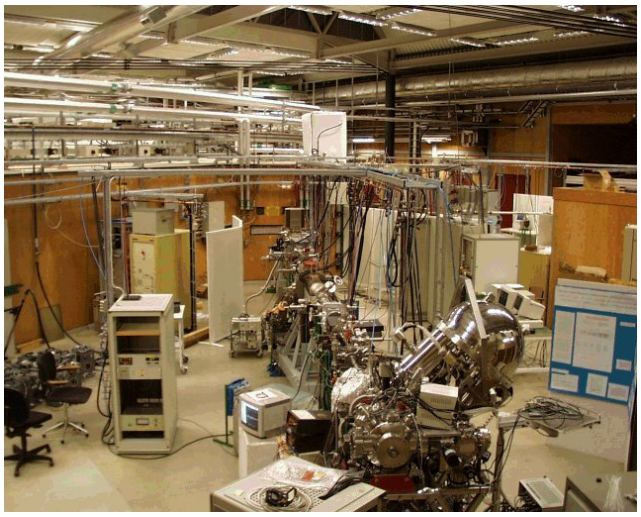

FIGURE 7 – *I411 beamline. This photo depicts, closest to the camera, the permanent analyzer chamber and hemispherical electron energy analyzer (not used in these experiments). In the background is the MAX II storage ring. [5]*

a drift tube with detectors in each end (see *figure 8* and). Light enters perpendicular to the drift tube into the extraction region, where the sample gas has been injected. If a molecule dissociates following ionization, there is at least one free electron and a corresponding ion. At the bottom of the spectrometer, an electron detector is placed. A positive charge is applied on the detector, attracting the free electrons. At the other end of the drift tube the ion detector is placed. A negative charge is applied in the acceleration region, thus accelerating the positive ions towards the ion detector. There is only an electric field present in the acceleration region. The potential in the drift tube is kept constant so the fragments have a free path.

Now, the electron detection acts as a time-starter and ion detection acts as a time-stopper. Given the mass ratio between the electron and typical ions, together with the great difference in path length, one can regard the electron detection as instantaneous, i.e. registered the same moment as the dissociation happens. Thus, the measured time interval measured is the TOF of the registered ion.

Since the spectrometer is a cylindrical structure, one can use cylindrical coordinates (z, r, ϕ) to describe its properties. Assume the fragmentation takes place at the origin, which we place in the middle of the extraction region. The z-axis is set along the drift tube. The center of the ion-detector is placed in $(\ell, 0, 0)$. The light enters the chamber along the $r\phi$-plane at $\phi_{in} = 160°$ with polarization vector along $\phi_{pol} = 70°$

3.3 Dissociation directions and 2D-detection

In the previous section I have discussed what happens to a charged fragment initially at rest. Assume now that a fragment directly after dissociation has a momentum $\mathbf{p} = \mathbf{p}_z + \mathbf{p}_r$. The electric field is applied along the z-axis, thus only giving rise to a change in $\mathbf{p}_z$. The $\mathbf{p}_r$-vector is undisturbed.

It has previously been stated that the time-of-flight for a particle initially at rest in

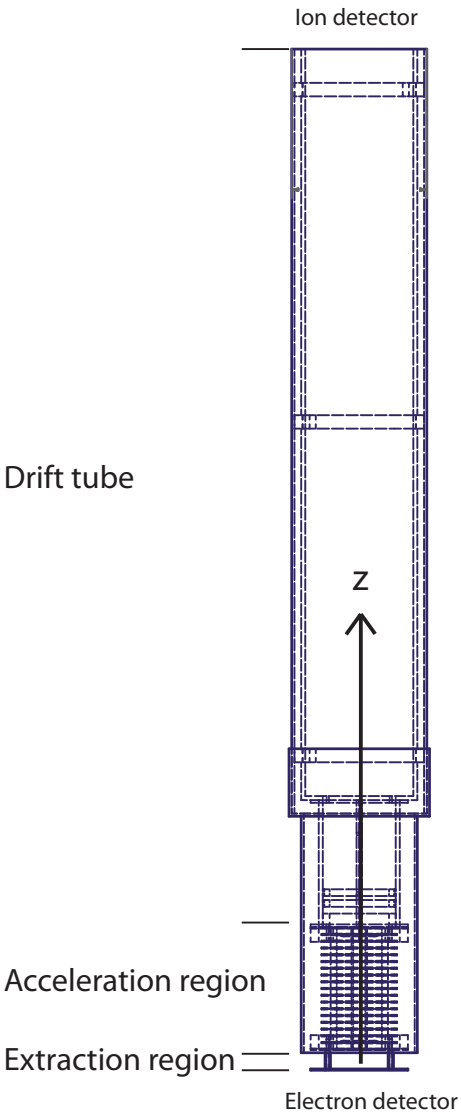

FIGURE 8 – *The TOF-spectrometer. Light enters the spectrometer in the extraction region where the gas also enters through a needle. The diameter of the region where the light meets the gas is 0.2 mm. Electrons are attracted by applying a positive potential (+440 V) on the electron detector. Ions enter the acceleration region where a negative potential has been applied such that a homogeneous electric field is directed towards the ion detector (diameter 80 mm). The different cathodes seen as layers in the acceleration region have increasing negative potential up to –4000 V. The drift tube and detector also has a potential of –4000 V, hence no acceleration takes place. The drift tube only serves as an intermediate region to make the TOF longer and thus making the fragments more distinguished.*

$h\nu$[eV]	Resonance
288.08	C $1s - \pi^*$
311.5	C $1s - \sigma^*$
286.0	below resonance

TABLE 1 – *Three sets of data have been acquired. Photon energies have been chosen in accordance with certain resonances found by examination of the NEXAFS-spectra in* figure 9. *Also at off-resonance case has been measured. Designations found in [8]*

the chamber is solely determined by the mass-to-charge ratio. The broadening of the peak and the peak-shape is determined by which directions and with which kinetic energies the fragments are emitted. The differences of time-of-flight within a peak are a measurement of the momentum along the z-axis (the detector axis). A long time-of-flight correspond to a momentum vector directed away from the detector ($p_z < 0$) and vice versa. Fragments with TOFs in the peak center thus has $p_z = 0$, hence either with almost zero kinetic energy or with a momentum vector in the plane perpendicular to the z-axis.

The p_r component of the fragment momentum is not possible to determine by TOF-measurements. The direction of the momentum does however affect the position of the fragment when it hits the ion detector. In this experiment this quantity can be measured since a 2D-detector has been mounted at the end of the drift tube. The term 2D-detector implies that it is able to measure the fragment's position in two dimensions x and y (or r and ϕ)

What determined if we know the values of r and ϕ when the fragment hits the detector? Since the only force applied to the fragment is the coulomb force directed along the z-axis, the ϕ-angle is completely undisturbed during the drift. The ϕ measured in the detector is thus the same as the ϕ which the fragment had directly after dissociation. The $\mathbf{p_r}$ vector is not affected, but the value of r is proportional to the TOF. However, since the differences of TOF within the peak are small compared to the total TOF, this perturbation can be neglected. One can regard the value of r as directly proportional to the initial value of p_r.

So, by measuring these values — TOF, radius in the detector and angle in the detector — one obtain full knowledge of the initial momentum vector $\mathbf{p}$.

3.4 Data

By core-excitation of OCS we promote one C 1s electron to an unoccupied valence state. The required photon energies thus lie just below the ionization threshold of the C 1s electron (the C 1s edge). To find exact resonance energies, absorption spectra are acquired. Absorption spectroscopy measures the probability for a photon to be absorbed by the sample. Since photons have higher probability to be absorbed at resonance energies, these are visible as peaks in the spectrum.

In the present paper, three sets of data are used. These are indicated in the *table 1* and the corresponding photon energies are marked in *figure 9*

The purpose to measure fragmentation in one σ- and one π-resonance (together with one non-resonant case) is to see differences between these cases.

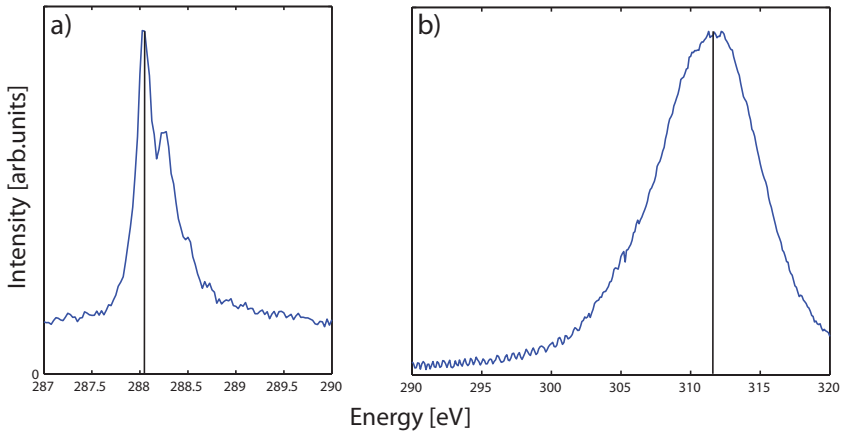

FIGURE 9 – *Absorption spectrum at the C 1s edge. a) The prominent* C $1s - \pi^*$ *peak. As seen, there are multiple vibrational states. The vibrational ground state is chosen. b)* C $1s - \sigma^*$ *give rise to this peak[8]. Note that the scaling on both the energy-axis and the intensity-axis are different. The vertical lines indicate the resonances used in this experiment (see* table 1*).*

4 Results and Analysis

4.1 The TOF-spectrum

In this paper, where the time of flight of molecular fragments plays a crucial role, it is important to know the relative masses of all possible fragments. In *figure 10* the complete time of flight spectrum following the C $1s - \pi^*$. All major peaks are identified.

One concern is that of isotope shifts in the TOF-spectrum. As the abundance of oxygen isotopes other than ^{16}O is just approximately 0.2 % of the total number of oxygen atoms, one can consider ^{16}O to be the only oxygen isotope. For carbon and sulfur however, two isotopes must be taken into consideration. The abundances of ^{13}C and ^{34}S are however fairly small (approximately 1 % and 4 % respectively). The isotopes are clearly visible in *figure 11*. To avoid having fragments of different mass, giving strange results since they have different TOF, I will in the following analysis always take only the fragments containing ^{16}O, ^{12}C and ^{32}S into consideration.

It could however be noted that the existence of isotope peaks is not only a concern, but can also be a help. When two peaks appear at the same TOF, the strength of isotope peaks can help us to extract the contribution from one fragment, if the ratio between isotopes is known. I.e. this effect can help us distinguish between O^+ and S^{++}.

The complete TOF-spectrum in *figure 10* is the first piece of data that can be analyzed. From the TOF-spectra, molecular fragments can be identified, and by the peak shapes a first analysis of spatial distribution can be done. As previously stated, fragments with a small mass-to-charge ratio appear in the left side of the spectrum, and vice versa.

Some differences between the two spectra. Most striking is the higher abundance

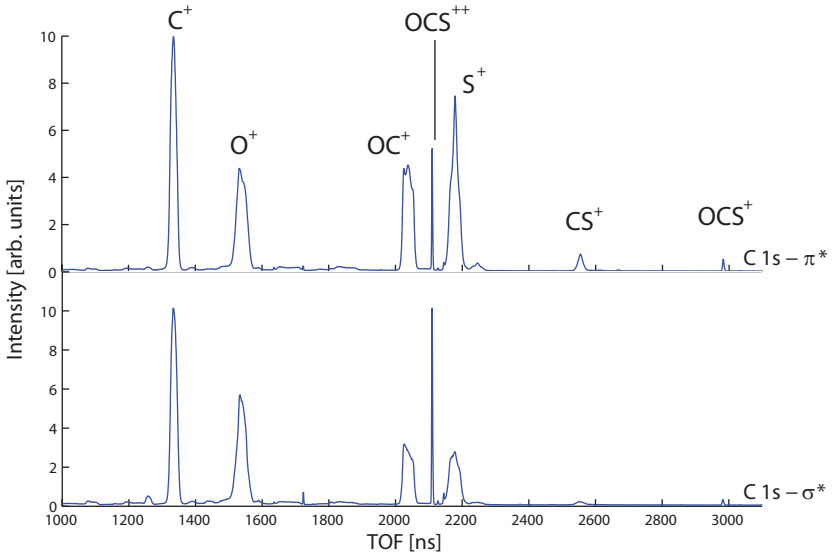

FIGURE 10 – *The complete time-of-flight spectrum recorded in experiments. Here the* C1s$-\pi^*$ *and the* C1s$-\pi^*$ *spectra. Peaks are identified by converting the TOF to mass-to-charge ratios.*

of the doubly charged OCS^{++}-ion. This can be explained by a higher photon energy in the σ-case.

The TOF-spectra of all experimental sets in this paper have the same prominent peaks. As intuitively expected one sees the singly ionized one-atom fragments C^+, O^+ and S^+. One also expects the singly ionized two-atom fragments OC^+ and CS^+. Also non-fragmented OCS-ions appear. These play an important role in determining the resolution of the spectrometer. In the present paper, I shall not discuss processes involving more exotic fragments. It should be noted however that a deeper search for less prominent peaks reveal doubly and triply ionized fragment. Also, the OS^+-ion appears in some cases, the production of which would be an interesting topic for another study.

4.2 Alignment

As previously mentioned these experiments have been carried out with 2D-detection. Thus we have the possibility to determine dissociation directions of the fragments in certain channels. In the next section I will focus on the z-dependence, i.e. time-of-flight. This section will concern with $r\phi$-dependence, i.e. the spatial distribution of fragments. To make a $r\phi$-plot is to make a picture of the 2D-detector and mark each place where a fragment has hit. Since the detector is perpendicular to the z-axis, it is also parallel to the synchrotron radiation beam. The synchrotron light has plane polarization in the same plane as the detector. The polarization vector is marked in *figure 14*. The O^+ peak has been sliced into three TOF-intervals seen in *figure 13*. The center interval (called *top*) includes the fragments which have almost zero initial momentum in the z-direction ($p_z \approx 0$), e.g. are ejected in the plane perpendicular to the z-axis. The left interval (called *left shoulder*) consists of fragments with less

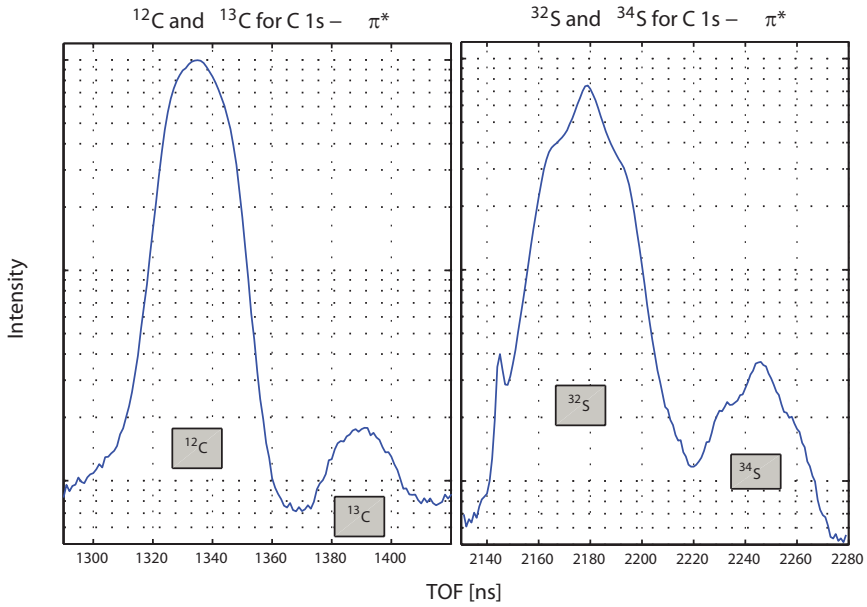

FIGURE 11 – *TOF-spectra showing the isotope dependence of the* C^+ *and* S^+ *(*$C1s-\pi^*$ *resonance). The plot is in logarithmic scale. As expected the abundances of* ^{13}C *and* ^{34}S *are approximately 1 % and 4 % respectively*

TOF, thus having initial momentum $p_z > 0$, and correspondingly the *right shoulder* consists of fragments with initial momentum $p_z < 0$.

In *figure 14* we observe a clear distinction between π- and σ-resonances. The clearest effect is seen in the *top* plots where the alignment effect is very striking.

Since dissociation reactions are very fast compared to the nanosecond time-scale in the spectrometer the dissociation direction is almost exactly the same as the alignment of the molecule upon absorption of the X-ray photon. *Figure 14* shows that excitation of C 1s electrons to the σ state is most probable if the OCS molecule is aligned parallel to the polarization vector. Also, excitation of C 1s electrons to the π state is most probable if the OCS molecule is aligned perpendicular to the polarization vector. This behavior is consistent with selection rules.

4.3 Comparison of O^+ and S^+

Chemically, oxygen and sulfur are much alike. In their atomic form they have the same set of valence orbitals (as they belong to the same group in the periodic system). The difference of OCS and e.g. CO_2 lays in the much larger mass and larger size of the sulfur atom than the oxygen atom. Bonding orbitals are the same in both the OC-bond and the CS-bond.

When a C 1s electron is promoted to a valence orbital it is a way to treat O and S equally. A core-hole is created in the middle of the molecule and the electron occupies an orbital that is stretching over the entire molecule.

In *figure 15* and *figure 16* I observe some striking differences between the behavior of the O^+ and S^+ fragments produced upon the $C1s - \pi^*$ excitation. The TOF peak is sharp for the S^+ ion, but has a plateau for the O^+ ion. This feature is seen in all C

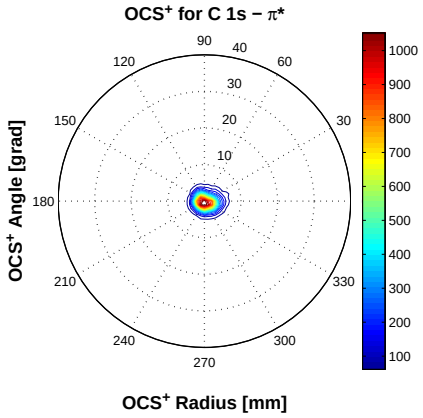

FIGURE 12 – *Resolution of the r ϕ-plot. Since the OCS^+ does not dissociate is cas be expected to have zero initial kinetic energy. Thus, it is a good fragment to use for calibration and resolution purposes.*

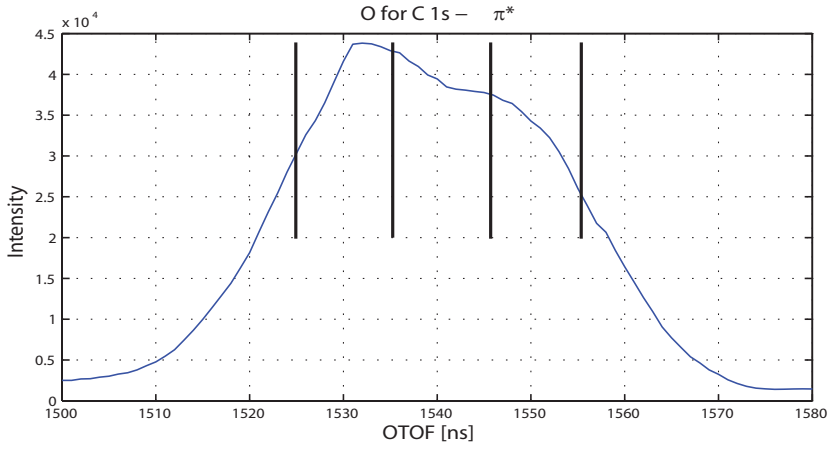

FIGURE 13 – *The O^+ peak has been sliced into three parts: (1) left shoulder:* 1526 – 1536 ns*, (2) top:* 1536 – 1546 ns*, and (3) right shoulder:* 1546 – 1556 ns*.*

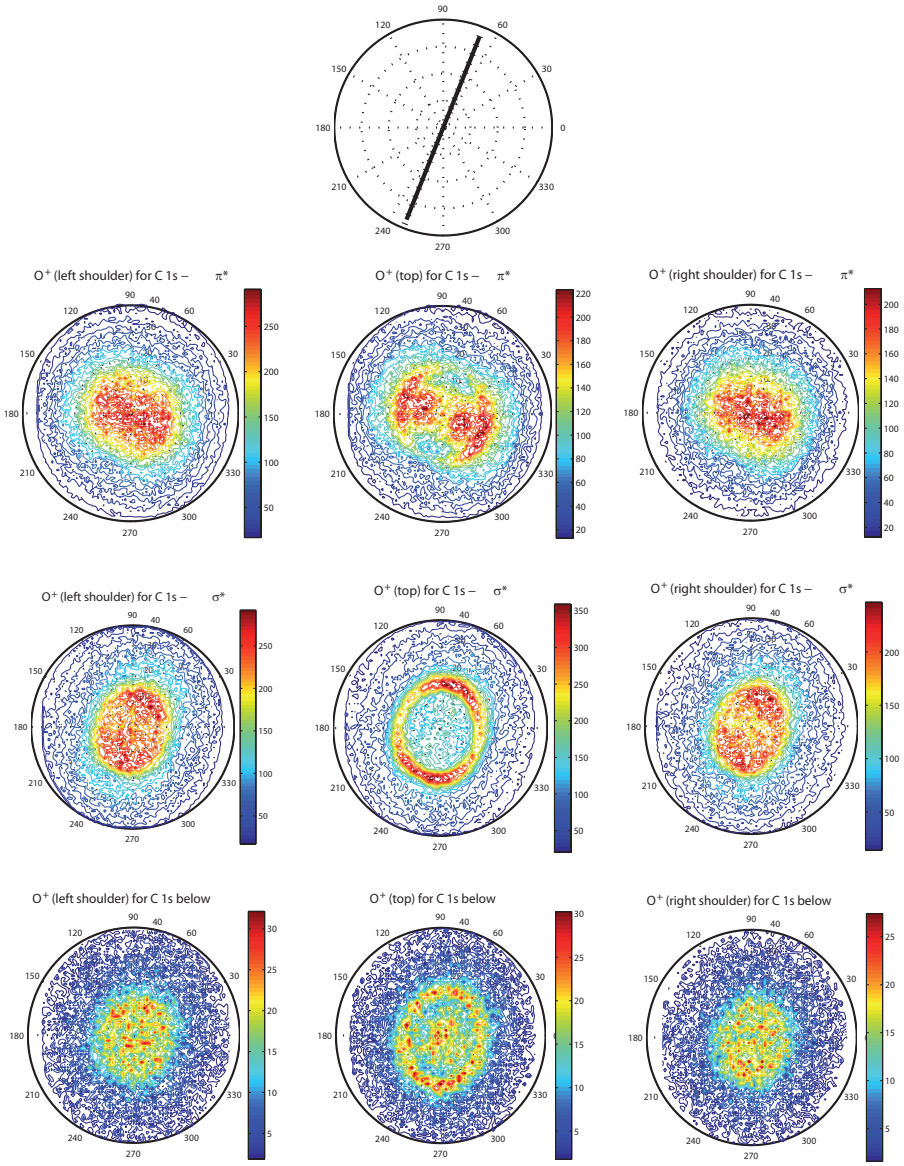

FIGURE 14 – *$r\phi$-plots of detected fragments in the O^+ peak. The peak has been sliced into three narrow TOF-regions each with a time interval of* 10 ns. *The O^+ peak has two shoulders and a slightly decreasing plateau in between. The three slices are seen in* figure 13. *The top plot shows the polarization direction of the incoming light. Then we have plots from the* C 1*s* $-\pi^*$, C 1*s* $-\sigma^*$ *and* C 1*s* below resonance *respectively.*

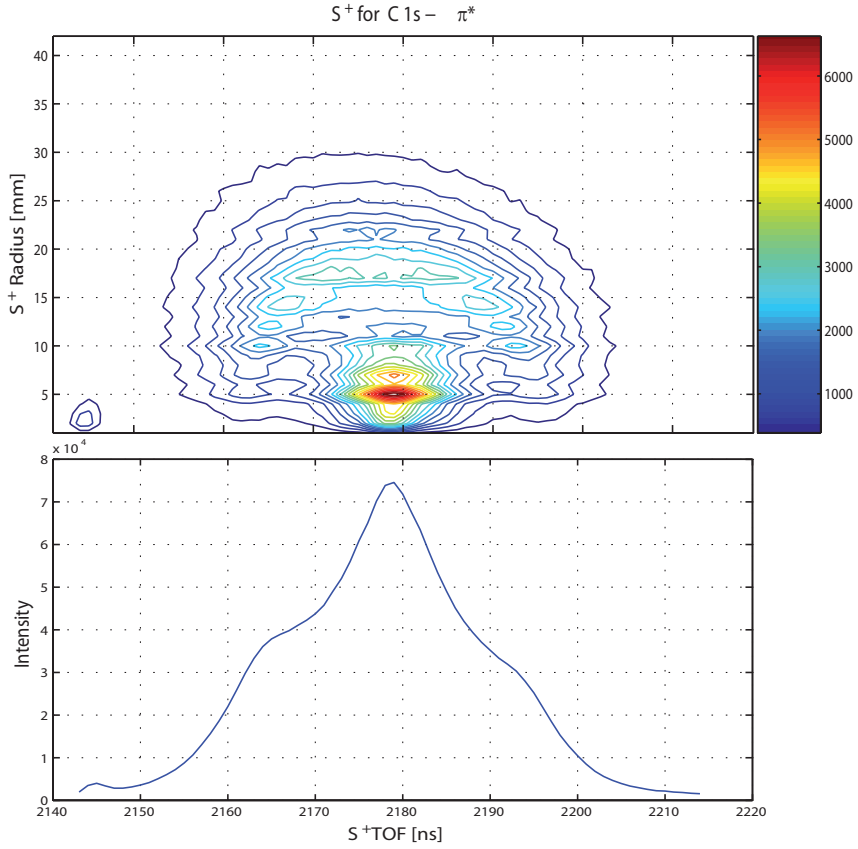

FIGURE 15 – *The S^+ fragments in* C 1*s* $-$ π^* *excitation. In the lower panel the peak shape is depicted (TOF plotted against the number of ions detected). A sharp central peak is observed, accompanied by a shoulder on each side. In the upper panel, radius is plotted against the TOF. One can clearly see that the fragments are distributed among two channels – the central maximum and the bent shape with a maximum radius of 18 mm.*

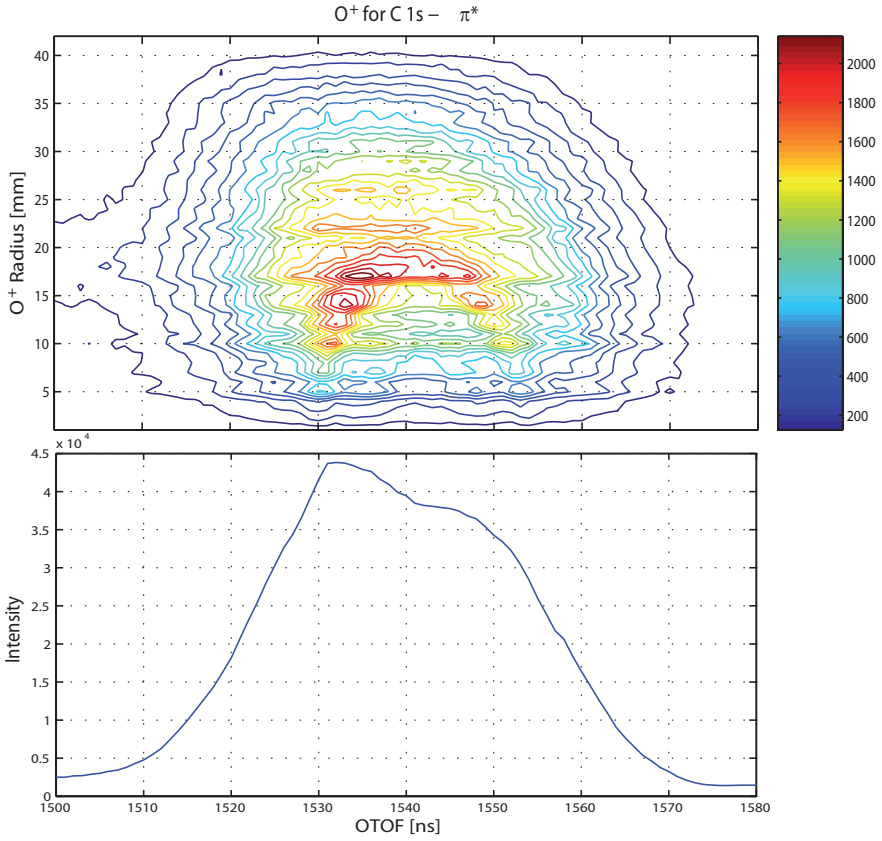

FIGURE 16 – *The O^+ fragments in* C 1*s* $-$ π^* *excitation. In the lower panel the peak shape is depicted (TOF plotted against the number of ions detected). In comparison with the S^+ peak in* figure 15 *there is no central peak. In the upper panel, correspondingly, there is no central maximum.*

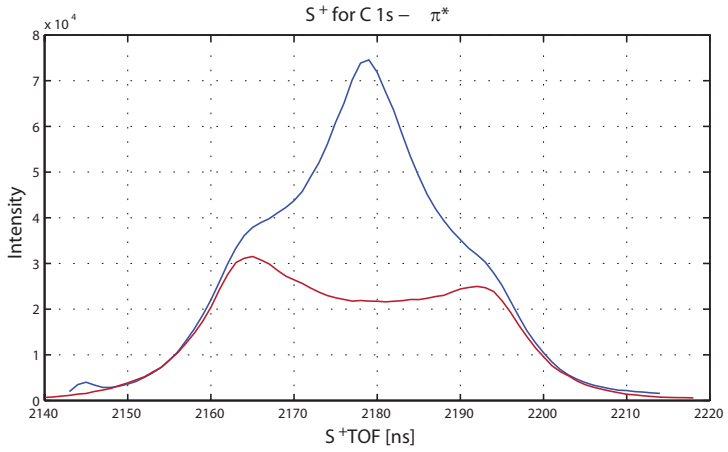

FIGURE 17 – *The graph (blue) depicts the S^+ fragments in* C 1*s* $-$ π^* *excitation. The subgraph (red) shows the fraction of all registered S^+ that come in coincidence with any other charged particle. We observe, in connection with* figure 15 *the correlation between high kinetic energy and coincidences with other charged particles.*

1s excitation data sets. The time-to-radius plot reveals why this is so. In the S^+ plot, two processes are clearly distinguishable. One of them is localized at the peak center with no radial change from the initial position, and thus no initial momenta. The other shape implies that these fragments have initial momentum, and presumably the same kinetic energy. In the O^+ plot only fragments with nonzero kinetic energy are observed.

If the electronic structure is such that there is no stable bond between them, they will move apart. When the nuclei have moved sufficiently far away the electrons will screen the nuclei and they will no longer feel each other. However, if they now both are positive ions they will continue to repulse each other, thus gaining kinetic energy in the dissociation direction. Presumably, in fragmentation processes where more than one charged fragment is produced the fragments would have higher kinetic energy.

In *figure 17* it is shown that the two channels seen in the S^+ peak are distinguishable and also that the fragments with high kinetic energy come in coincidence with other charged particles.

Since O^+ obviously does not come in coincidence with neutral particles some decay channels can be excluded

$$\begin{aligned} OCS^+ &\rightarrow O^+/CS \\ OCS^+ &\rightarrow O^+/C/S, \end{aligned}$$

although we have clear evidence that as least one of the corresponding processes is prominent

$$\begin{aligned} OCS^+ &\rightarrow OC/S^+ \\ OCS^+ &\rightarrow O/C/S^+. \end{aligned}$$

Resonance	C^+	O^+	S^+	OC^+	CS^+	*Noise*		O^+/CS^+	OC^+/S^+
C $1s-\pi^*$	25.0	19.3	23.0	18.2	1.9	*9.2*		1.5	20.3
C $1s-\sigma^*$	27.1	24.2	13.4	13.3	1.4	*14.6*		0.7	16.0
below resonance	16.1	23.9	20.9	13.0	1.8	*13.0*		1.1	20.0

TABLE 2 – *Branching-ratios for the five singly ionized fragments and for the dissociation into two singly charged fragments. The branching ratios are, in the one-particle case, the percentage of the total number of detected fragment. In the two-particle case it is the percentage of the total number of two-particle coincidences. The Noise column shows the percentage of the detected fragments that could not be assigned to a peak.*

There obviously exists a factor that allows for the CS bond to break without putting a charge on the sulfur atom, which does not exist for the OC bond.

In connection with this I have studied the branching ratios[7] of the possible outcomes when OCS dissociates into two singly charged fragments[8]. In *table 2* branching-ratios of different fragments are listed.

It stands very clear that the $OCS^{++} \rightarrow OC^+/S^+$ channel is more favored than the $OCS^{++} \rightarrow O^+/CS^+$ channel. As we have seen that the channel $OCS^+ \rightarrow O^+/CS$ is non-existing, one must draw the conclusion that it is more favorable to break the CS bond than the OC bond.

We get an idea of the different bond strengths by noting that the diatomic molecule CO has in its ground state dissociation energy of 11.09 eV, while CS has 7.36 eV [9].

Another aspect is the difference in electronegativity between the oxygen and the sulfur atom. Oxygen has a considerably higher electronegativity than both sulfur and carbon. This would imply first that oxygen tends to keep electrons to itself, but also that it has a higher ability to attract other electrons. The C 1s excitation does not obstruct any particular bond. However, since oxygen tend to attract electrons more than sulfur it is possible that the ionization is more likely to take place close to the sulfur end. This would have a major effect on the CS bond. This explanation is also consistent with the non-existence of the channel $OCS^+ \rightarrow O^+/CS$ since it would require the sulfur end of the molecule to be preferred in attracting the electron. This behavior is also seen in the branching-ratios of the two-atom fragments where OC^+ has a considerably higher abundance than the CS^+.

There are some differences of the branching-ratios when one considers the three different resonances. There are increasing abundance of the C^+ ion when the photon energy is increased. C^+ is produced when the OCS molecule dissociates into three fragments[9]. One would expect that if one puts more energy into a system, it would be a higher probability for it to dissociate into more fragments, but also other effects could be occurring. We observe a higher abundance of S^+ and OC^+ fragments in the π resonance than in the σ resonance. Note that the number of "bad data" is higher in the σ resonance.

[7] In this text the brancing ratio is defined by counting the total number of fragments recorded in one peak and divide it by the total number of counts over all TOFs.

[8] It is only possible to do this calculation if both fragments are charged. It is not possible to make a direct branching-ratio calculation of channels which include one or more un-charged fragments.

[9] In principle the channel $OCS^{++} \rightarrow C^+/OS^{(+)}$ can occur. This is not expected since it would require a deformation and bending of the molecule before dissociation. The transitions dealt with in this paper are close to symmetric with respect to the molecular axis, why this would be very improbable.

5 Conclusion

This report has presented, interpreted and discussed some data concerning the C 1s core-electron excitation of molecular OCS. I am able to show some results regarding the bond strength and alignment effects. Now, the time which I have had the opportunity to work with this subject has been limited. This by no means are the sole results one can aquire from OCS, and there are many possible ways to further pursue this subject.

A natural way to continue is to repeat the analysis made at the C 1s edge with data aquired at the O 1s edge. It is possible that a lozalized core-hole in the oxygen atom would affect the branching ratios of the channels involving oxygen atoms and ions.

Alignment effects could be further examined by analysis of the two-atom fragments OC^+ and CS^+. One would expect similar effects as with the one-atom fragments.

As has been previously noted, the production of OS-fragments seam to be an exotic decay channel for OCS. It would be interesting to study this further in connection with examination of different vibrational effects.

References

[1] Karlsson, L. and Andersson, S., *Atom- och molekylfysik*, (Department of Physics, Uppsala University, 1999), pp. 107*ff*

[2] Atkins, P.W., *Molecular Quantum Mechanics 2nd ed.*, (Oxford University Press, Oxford, 1983), pp. 252*ff*

[3] Hollas, J. M., *Modern Spectroscopy 3rd ed.*, (John Wiley & Sons Ltd., Chichester, 1996), pp. 279-283.

[4] Lindgren, A., *Ion Spectroscopic Measurements on photo-aligned small molecules*, (MediaTryck, Lund University, Lund, 2006), pp. 8-10

[5] MAX-lab official homepage, *http://www.maxlab.lu.se/* , (2009-05-20)

[6] Lindgren *et al.*, J. Chem. Phys. **122**, 114306 (2005)

[7] M. Magnuson, J. Guo, C. Såthe, J.-E. Rubensson, and J. Nordgren, *http://www.als.lbl.gov/als/compendium/AbstractManager/uploads/magnuson.pdf*

[8] Sham *et al.*, Phys. Rev. A **40**, 652 (1989)

[9] Herzberg, G., *Molecular Spectra and Molecular Structure, IV. Constants of Diatomic Molecules* (Van Nostrand Reinhold Company, 1979), pp. 198 & 184